Building Tomorrow's Society
Bâtir la Société de Demain

Fredericton, Canada
June 13 – June 16, 2018/ *Juin 13 – Juin 16, 2018*

PERFORMANCE-BASED WIND DESIGN OF TALL BUILDINGS – WIND LOADING POINT OF VIEW

Jeong, Un Yong[1,4], Tarrant, Kevin[2] and Ferraro, Justin[3]
[1] Gradient Wind Engineering Inc., Canada
[2] Gradient Wind Engineering Inc., Canada
[3] Gradient Wind Engineering Inc., Canada
[4] unyong.jeong@gradientwind.com

Abstract: Tall buildings are vulnerable to wind loading, and their designs are therefore frequently governed by wind loads. ASCE 7 is moving toward implementing performance-based wind design for buildings. This paper addresses basic issues in applying performance-based design (PBD) to tall-building wind design by investigating different characteristics between wind loading and seismic loading. The main differences lie in: i) the probabilistic distribution of winds and ground accelerations, ii) aerodynamic effects such as vortex-shedding, and iii) the substantially longer duration of wind loading compared to that of earthquake loading. Potential benefits of performance-based wind design were investigated by comparing wind loads with seismic loads for various return periods. In order to derive general discussions and conclusions, the study was applied to a generic tall building with a square plan dimension of 30 m by 30 m, a building height of 300 m, and an aspect ratio (slenderness ratio) of ten (10). The across-wind and along-wind loads and their responses were simulated for a range of return periods, covering service level, strength level and collapse-prevention level events. Findings concluded that the 'heavy-headed, light-tailed' probabilistic distribution of wind speeds and singular building aerodynamic characteristics, as well as stiffness degradation due to long-duration wind loading, should be properly addressed for successful implementation of PBD to tall building wind design.

1 INTRODUCTION

Performance-Based Design (PBD) has been applied to wind design of tall and mid-rise buildings (Griffis et al. 2012; Larsen et al. 2016; Judd and Charney 2016; Nakai et al. 2013) in result of its potential advantages in providing economically feasible building seismic design. The key component of performance-based seismic design (PBSD) lies in finding a realistic design solution which satisfies both strength level in elastic material range and ultimate level (collapse-prevention level) by allowing post-yielding hysteretic behavior of materials (FEMA 2012; PEER 2010).

Performance-based wind design (PBWD) has been suggested to overcome the drawbacks (usually conservative design) of the current building wind design practice based on allowable stress design (ASD) and/or load resistant factored design (LRFD) by explicitly satisfying performance levels set out for different level of probabilities and intensities (Griffis et al. 2012; Larsen et al. 2016; Judd and Charney 2016). According to these publications, the main efficiency of PBWD can be achieved by allowing the post-yielding behavior of materials for collapse-prevention level winds which correspond to 700-year up to 20,000-year return periods for Risk Category II buildings. Regardless of some differences in defining target return periods, the suggested procedures are similar and are in line with those of PBSD.

For the successful implementation of PBWD, a couple of main issues should be properly addressed despite the generally agreeable arguments provided by the aforementioned studies, especially regarding the introducing post-yielding behavior of materials for extreme wind events at collapse-prevention level. Since tall buildings are governed by vortex-shedding, which usually increases rapidly up to the strength level wind loads and mildly increases thereafter, a building designed in elastic range for the strength level wind loading will remain elastic even for much higher return periods of collapse-prevention level wind loading. This implies that key benefit of PBWD using post-yielding behaviour of materials will be difficult to be applied to tall building wind design. Another issue is that the difference in degree of extremity between winds versus earthquakes. Earthquakes appear to be more extreme in intensity than winds. In consideration of the above characteristics of wind loads on tall buildings, the feasibility study on PBWD presented in this paper was performed by quantifying the statistical and aerodynamic characteristics of wind loading.

The following sections acknowledge several relevant considerations for this study: the main components of PBD are identified; probabilistic distributions of wind loads are compared to the earthquake loads; wind loading on tall buildings are decomposed in to along-wind and across-wind directions and compared with the seismic loads, and; wind loading characteristics in along-wind, across-wind are described in relation to PBD. Subsequently, using a typical tall building example, the main components of PBWD are discussed and compared to those of PBSD to examine the feasibility of expected material-saving effects of PBWD.

2 COMPONENTS OF PERFORMANCE-BASED DESIGN

Regardless of some issues in its application, PBD has demonstrated potential advantages in recommending reductions to reinforcements for new constructions and for repairs/replacements to existing buildings by optimally satisfying performance demands such as serviceability, strength and collapse-prevention. Although the performance objectives can be somewhat optimized between the serviceability and strength levels based on PBSD, the main efficiency of PBSD resides in allowing ductile behavior of structural members to prevent the subject building from total collapse under devastating earthquakes which have extremely low probability of occurrence, while still satisfying the strength requirements under much more frequent but smaller scale earthquakes.

Seismic load can be identified as a combination of an earthquake intensity and a dynamic transfer function of the structure, whereas wind load can also be identified as the combination of wind intensity, and dynamic and aerodynamic transfer functions. Whereas earthquake intensity is defined for a site in terms of a ground acceleration, wind intensity is mainly defined by the wind speeds measured on-site. Unlike the seismic loads, wind loads involve aerodynamic transfer functions due to the vortex shedding or motion-induced aerodynamic forces (self-exited forces), etc. Hereafter, the noted differences between wind and seismic loads will be discussed in detail.

3 WIND AND SEISMIC INTENSITY AND DURATION

Probabilistic distribution of seismic intensity (in terms of the design response spectrum at a given period) is characterized by ‘light head’ and ‘heavy tail,’ which means frequent seismic events are very low intensity, whereas extreme rare events are very high intensity. Figure 1 illustrates probabilistic distribution of seismic intensity (FEMA 2012; ASCE 2010) compared to wind (pressure) distribution based on statistical analysis of wind speed data (NOAA) in Seattle, WA, as an example. In the graph, the seismic intensity and dynamic wind pressure are normalized by 50-year values for the comparison. Probabilistic distribution of seismic loads can best be represented by lognormal distribution (FEMA 2012) with typical dispersion, β = 0.4 to 0.5, whereas wind pressure distribution is evaluated from the wind speeds (NOAA) for which distribution typically follows Type-1 Gumbel distribution. Figure 1 represents the differences between frequent event and the extreme event, which correspond to the low and high non-exceedance probability respectively; these differences are much larger for the seismic load than for the wind load, due to the light head and heavy tail characteristic of the seismic loads probabilistic distribution.

Wind events have much longer duration than seismic events, which makes PBWD more difficult than PBSD due to the significant degradation of the material (FEMA 2009) which will occur during the long-duration excitation.

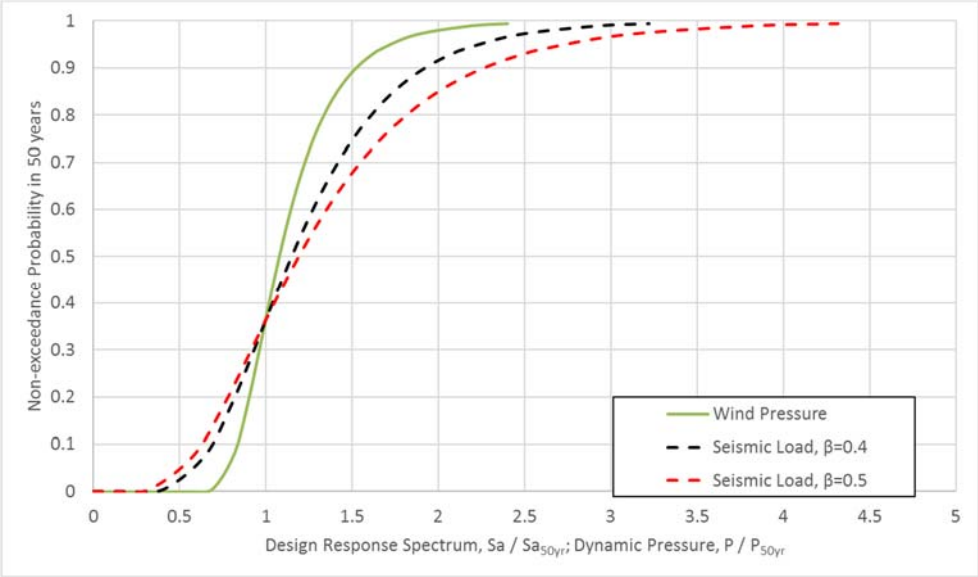

Figure 1: Non-exceedance probability of seismic and wind loads intensity normalized by 50-year values based on statistical analysis of wind speed data (NOAA), seismic intensity (ASCE 7-10) in Seattle, WA and probabilistic distribution (FEMA, 2012)

4 WIND LOADING ON TALL BUILDINGS

Tall buildings are susceptible to winds due to their flexibility and slenderness. The main sources of wind loading on tall buildings are vortex shedding, wind-buffeting and wake buffeting. Wind buffeting and wake buffeting are generated by boundary-layer wind turbulence and vortices shed from upstream buildings, respectively. When the wind loads on tall buildings are decomposed into along-wind and across-wind components, wind buffeting, vortex shedding, and wake-buffeting act in the along-wind, across-wind and both directions, respectively. Torsional wind load and wake-buffeting are not addressed in this paper due to relative insignificance in tall buildings and case-dependency, respectively.

As a building becomes taller and more slender, due to the increasing flexibility and susceptibility to resonance, building response rapidly increases until it reaches a level where the motion-induced wind force (aeroelastic force) becomes significant. While along-wind aerodynamic damping can be estimated to be positive, which gives favorable effects (Davenport 1979; Holmes 1996, 2001), across-wind aerodynamic damping can be either positive or negative around the vortex-shedding wind speed. Even though this issue is important in tall building wind design, this is not addressed in the current paper because it would not change the major points which will be discussed in relation to the performance-based design. However, the author has addressed these issues and its time-domain analysis formula in another paper (Jeong 2015).

On another note, wind events have much longer duration than seismic events, which makes PBWD more difficult than PBSD due to the significant degradation of the material which will occur during the long-duration excitation.

4.1 Along-wind Wind Loading

Along-wind response on a tall building consists of mean plus dynamic loads, which is a combination of quasi-steady load and resonant load. Since the along-wind load spectrum has close-to-uniform distribution, the along-wind response increases quadratically with respect to wind speed. The estimation of the dynamic

component of the along-wind loading of a building is generally obtained using the gust factor approach which has been utilized in several building codes. The basis of the gust factor approach follows from Davenport's method (Davenport 1964) whereby the maximum along-wind displacement $\hat{Y}$ can be expressed as:

[1] $\hat{Y} = G\,\bar{Y}$

where $\bar{Y}$ is the mean static displacement and G is the gust factor, expressed as:

[2] $G = 1 + g_y \frac{\sigma_y}{\bar{Y}}$

where g_y is the peak factor and σ_y is the standard deviation of the fluctuation around the mean displacement. Details of the method to calculate G in this paper can be found in the work by Solari (Solari 1993a, 1993b). It has been assumed in the analysis that the fundamental mode primarily contributes to the building response.

4.2 Across-wind Wind Loading

Since the across-wind load spectrum has a peak around the 7 to 15 second period due to the vortex shedding, across-wind response of tall buildings whose natural periods fall within 5 to 10 seconds drastically increases due to resonance. As building height increases, vortex shedding wind loads increase rapidly, since the vortices and their shedding frequencies are highly correlated along the vertical axis of the building. Conversely, the along-wind buffeting loads increase moderately due to the relatively low correlation of boundary layer wind turbulence along the tower height. The power spectral density (PSD) of the across-wind displacement response, $S_{\tilde{x}}$ can be calculated as follows based on random vibration theory for stationary processes (Clough and Penzien, 1993, Jeong 2015):

[3] $S_{\tilde{x}} = \widetilde{m}^{-2} {k_m}^2 |h(\omega)|^2 S_M(f)$

where $\widetilde{m}$ is the generalized mass that equals to $\int_0^H \phi_{x1}^2 m\,dz$; H is building height; ϕ_{x1} is the first across-wind directional mode shape function which is approximated with $\phi_{x1} = (z/H)^{\mu}$;m= mass per unit height;

[4] $k_m = \frac{\int_0^H \phi_{x1} p(z) dz}{\int_0^H z p(z) dz}$;

[5] $h(\omega) = [(-\omega^2 + {\omega_1}^2) + i(2\xi_1 \omega_1 \omega)]^{-1}$;

$p(z)$ denotes the wind load distribution along the height; $S_M(f)$ is the PSD of the base bending moment which can be calculated according to AIJ (AIJ 2006; Jeong 2015). The variance of the across-wind acceleration response of the building is:

[6] ${\sigma_{\ddot{x}}}^2 = \int_0^{\infty} S_{\ddot{x}} df$

The shear force and bending moment at a location $\alpha H, (0 \le \alpha \le 1.0)$, along the building height can be respectively expressed as:

[7] $F(z) = \frac{mBD}{H^{\mu}} {\sigma_{\ddot{x}}}^2 \int_{\alpha H}^{H} z^{\mu} dz$

[8] $M(z) = \frac{mBD}{H^{\mu}} {\sigma_{\ddot{x}}}^2 \int_{\alpha H}^{H} z^{\mu} (z - \alpha H) dz$

where m represents the mass density of building.

5 SEISMIC RESPONSE OF TALL BUILDINGS

In the formulation of seismic response of tall buildings, the effect of higher modes can have a significant influence on the overall response when compared to that of the first mode response. Neglecting the effect of higher modes can lead to unconservative results. The equation of motion of a tall building subjected to ground acceleration $\ddot{x}_g(t)$ is given by:

[9] $\ddot{\tilde{x}}_j + 2\xi_j\omega_j\dot{\tilde{x}}_j + {\omega_j}^2\tilde{x}_j = -\frac{\tilde{L}_j}{\tilde{m}_j}\ddot{x}_{gj}(t)$

where $\tilde{x}_j$ is the generalized coordinate of the *j*th mode and $\tilde{L}_j\ddot{x}_{gj}(t)$ is the generalized excitation with:

[10] $\tilde{L}_j = \int_0^H m(z)\phi_{xj}(z)dz$

and $\phi_{xj}(z)$ is the mode shape for mode *j* in the *x*- direction. To compute the bending moments and shears associated with the displacement $x(z,t)$, the method of equivalent static forces has been used. These forces are defined as the external forces that would cause displacements $x(z)$ defined by Chopra (Chopra 1995) as:

[11] $f_{oj}(z) = \frac{\tilde{L}_j}{\tilde{m}_j}m(z)\phi_{xj}(z)S_{ai}$

where S_{ai} is the ordinate of the acceleration design spectrum at a given period. The value of spectral acceleration is assumed to be lognormally distributed with median value θ, and dispersion β, and can be obtained according to FEMA P-58-1 (FEMA 2012) as:

[12] $S_{ai} = \theta e^{\beta\Phi^{-1}(P_i)}$

where Φ^{-1} is the inverse standardized normal distribution, and P_i is the midpoint cumulative probability for region *i* within the interval used to characterize the distribution of seismic demand. Thus, the shear and bending moment at a height $\alpha H, (0 \le \alpha \le 1)$ can be respectively expressed as:

[13] $F_j(z) = \int_{\alpha H}^H f_{oj}(z)dz;$

[14] $M_j(z) = \int_{\alpha H}^H f_{oj}(z)[z - \alpha H]dz$

for mode j. The contribution of each mode to the overall response is determined by combining the maximum effect of each mode to the response using the square root of sum of squares (SRSS) method.

6 EXAMPLE – DESIGN LOADS FOR PERFORMANCE-BASED DESIGN OF A TALL BUILDING

A tall building with a building height, H, of 300 m, with uniform square-shaped floor plates with dimensions of 30 m (B) × 30 m (D) was analyzed in along-wind and across-wind directions for various wind speeds that corresponded from weekly to 10,000-year return period wind speeds in Seattle, Washington. The wind exposure applied was the open exposure which has turbulence intensity of approximately 10% at the building height based on ASCE (2010) and ESDU (1984). The mass density of the building was 225 kg/m^3; the mass per unit height was equal to 202.5×10^3 kg/m. Figure 2 illustrates the building's natural vibration modes and corresponding frequencies and periods for the first six modes in the direction of interest. The building's first mode frequency and structural damping ratio were 0.1 Hz (i.e., building period, T = 10.0 s) and 0.02 respectively. For the 1st mode, the exponent of the mode shape, μ, was 1.5 which is a typical value for tall buildings, where mode shape function, $\phi = (z/H)^{\mu}$, where z is elevation from the ground.

According to wind speeds measured at King County International Airport in Seattle, 50-year return period mean hourly wind speeds in Seattle at 10-meter height in open exposure is 25 m/s, which corresponds to 85 mph 3 second gust wind speed according to ASCE 7-05 (ASCE 2005). The empirical across-wind

spectrum (AIJ 2006) has been used in this example due to the simplicity and versatility. Figure 3 illustrates across-wind spectrum in terms of base moment, as well as the vortex shedding peak value occurring around the reduced frequency ($f_s B/U_H$) of 0.1 typical for buildings with a square plan (Gu and Quan 2004; Chen et al. 2014).

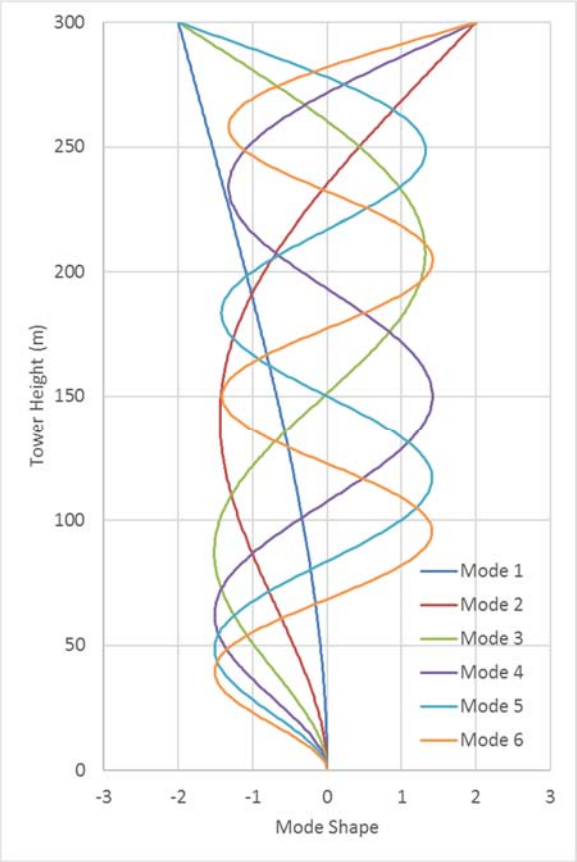

Mode	Frequency (Hz)	Period (sec)
1	0.100	10.0
2	0.627	1.60
3	1.755	0.57
4	3.439	0.29
5	5.685	0.18
6	8.492	0.12

Figure 2: Natural vibration modes of the building

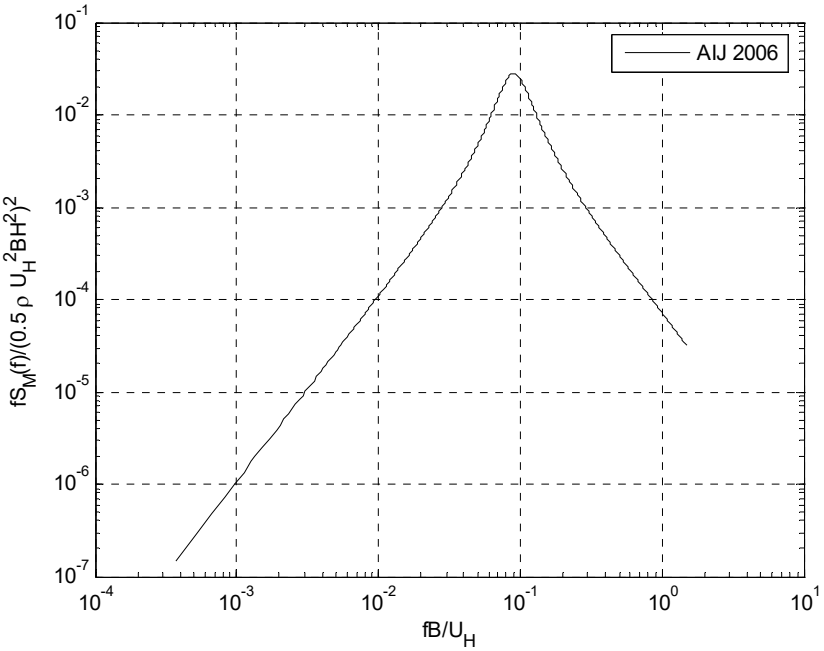

Figure 3: Normalized base moment spectra of the subject building based on AIJ (2006)

For the comparison, seismic loads were also estimated in terms of response spectrum according to ASCE 7-10 (ASCE 2010). Based on USGS Design Map (ASCE 7-10) as illustrated in Figure 4, the Design Spectral Acceleration Parameter, S_{D1}=0.348 g; long-period transition period, T_L= 6 seconds; and corresponding Design Response Spectrum, $S_a = S_{D1}T_L/T^2$ = 0.02088 g for collapse probability of 1% in 50-year in Seattle (ASCE 7-10). The above values were achieved by assuming Site Class-B and Risk Category I, II and III. The distribution of the seismic intensity was assumed to be a lognormal distribution with dispersion coefficient, β, of 0.4 to 0.5 which is a typical statistical distribution of seismic intensity (FEMA 2012). Figure 1 illustrates the probabilistic distribution of the seismic intensity for the different dispersions of 0.4 and 0.5.

Base moments during vortex-shedding (across-wind direction) and wind-buffeting (along-wind direction) were evaluated based on spectral analysis and gust buffeting theory (Solari 1993a, 1993b), respectively. In the wind analysis, only the first mode was considered since the higher mode contributions were minimal. The peak base moments were represented in Figure 5. As shown in the figure, the across-wind loads drastically increased from 1-year to 10-year return periods; however, the slope quickly reduced after 50-year return period and maintained a very mild slope beyond this point. As briefly mentioned above, those high across-wind responses were due mainly to the vortex-shedding. However, along-wind loads quadratically increased and reached the level of the across-wind load for 10,000-year return period. The example represents a typical tall building behavior which is governed by the across-wind vibration.

Base moments were also calculated for the above seismic loads, considering the 6 lowest vibration modes. Based on the assumption of uniform mass density, the base overturning moments were calculated using the inertia forces of the modes which were combined based on SRSS method. As shown in Figure 5, the overall base moment caused by seismic loads were much lower than those caused by wind loads over the serviceability and strength levels, because of the long fundamental building period (low building frequency).

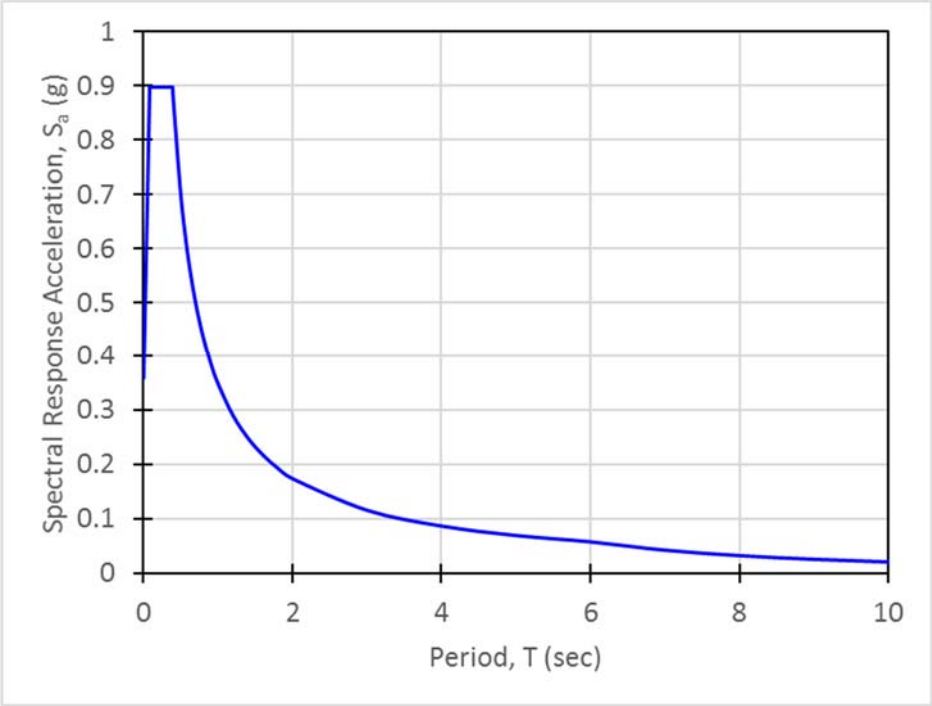

Figure 4: Design Response Spectrum at the Project Site, Seattle, WA (ASCE 7-10)

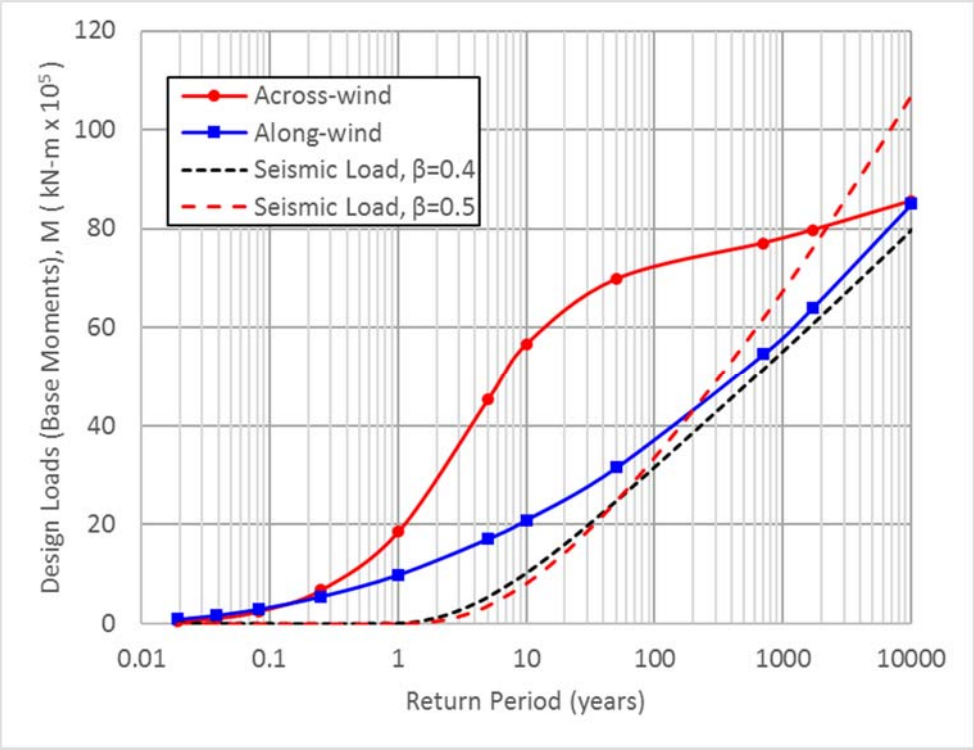

Figure 5: Peak base moment for various return period under wind and seismic loads

For the PBWD, 1-year and 10-year accelerations were limited by the industry guidelines for the serviceability; 50-year wind load for strength required the structure remain in an elastic state; 10,000-year wind load for collapse-prevention demand allowed plastic deformation of some elements (Judd and Charney 2016; Larsen et al. 2016). As shown in Figure 5, the collapse-prevention level loads (say, 10,1000-year return period) were 3.2 to 4.3 times larger than the strength level (50-year return period) for seismic loads; whereas only 2.7 and 1.2 times for along-wind and across-wind loads, respectively. For the seismic loads, the structural materials could be saved by allowing plastic deformation to dissipate large seismic energy without substantial reinforcement for very high collapse-prevention level seismic loads, while keeping the structure in the elastic range up to the strength level loads. Furthermore, as briefly mentioned in the introduction, the ductile design is applicable for seismic loads because the short-duration of the seismic loads prevents complete collapse from the cyclic degradation (FEMA 2009). However, for the across-wind loads, the difference between the collapse-prevention level and the strength level loads is too small to allow ductile behavior of the material while keeping it elastic for the strength level loads, which means the material will always remain in elastic range.

Although the main goal of this paper is to address the issues related to performance objective optimization between the strength and collapse-prevention levels, there may be more potential efficiency of PBWD in optimizing the levels of serviceability and strength levels (Nakai et al. 2013; Griffis et al. 2013). To investigate the wind issues for these levels, the peak accelerations in across-wind and along-wind directions were evaluated, and the results were compared for service level winds. As shown in Figure 6, the across-wind response governed the serviceability condition due to the vortex shedding. Since the building accelerations were estimated to substantially exceed the industry guidelines (ISO; Isyumov 1993, 1995), artificial damping such as Tuned Liquid Sloshing Damper (Kareem 1987, 1990; Jeong 2015) or Tuned Mass Dampers will be required for the building to mitigate the excessive vibrations to the acceptable levels. Artificial dampers also affect the building performance and will be investigated in future research by the authors.

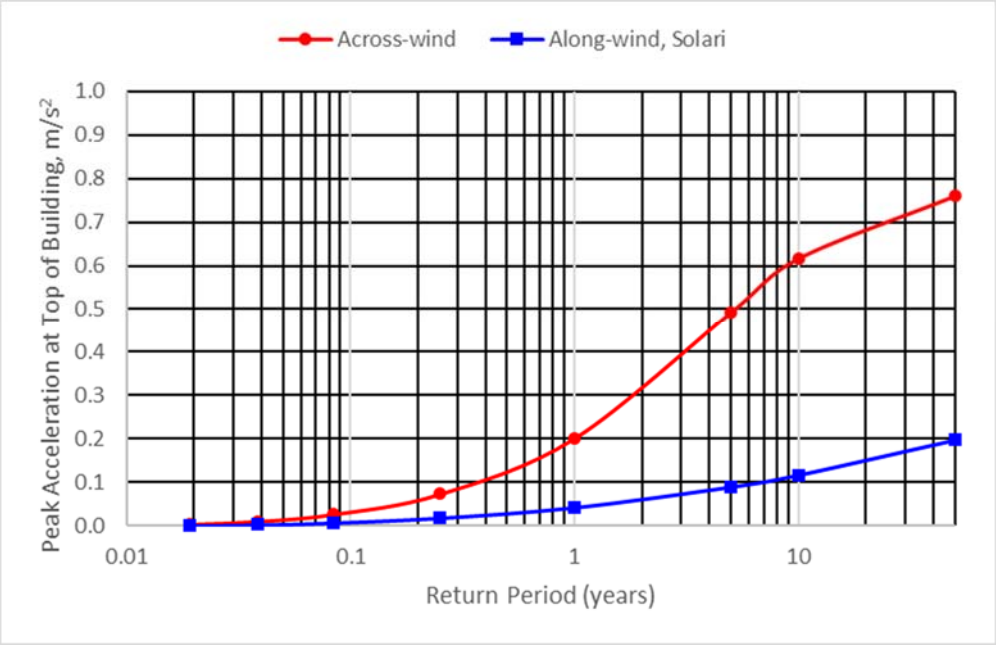

Figure 6: Peak accelerations at top floor for various return periods

7 CONCLUSIONS

Wind design of tall buildings were investigated in consideration of PBD. Tall slender buildings were governed by the across-wind loads which very slowly increased beyond the strength level wind loads even in much longer return periods. This important characteristic of wind loads should be properly addressed

together with other issues such as long-duration, and probabilistic distribution of wind speeds for the successful application of the conventional PBD approach to tall building wind design. There is potential efficiency of PBWD in optimizing the levels of serviceability and strength levels, by calculating building drifts explicitly as well as considering the effects of supplemental dampers in structural design.

References

American Society of Civil Engineers (ASCE). 2005. Minimum design loads for buildings and other structures, ASCE Standard ASCE/SEI 7-05.

American Society of Civil Engineers (ASCE). 2010. Minimum design loads for buildings and other structures, ASCE Standard ASCE/SEI 7-10.

Architectural Institute of Japan (AIJ). 2006. Recommendations for loads on Buildings.

Chen, X., Kwon, D. and Kareem, A. 2014. High-frequency force balance technique for tall buildings: a critical review and some new insights. Wind and Structures, 18(4): 391-422.

Chopra, A.K. 1995. Dynamics of Structures, Pearson.

Clough, R.W. and Penzien, J. 1993. Dynamics of Structures – 2nd edition, McGraw-Hill International Edition.

Davenport, A.G. 1979. The Influence of Turbulence on the Aeroelastic Responses of Tall Structures to Wind. IAHR-IUTAM Symp. Pract. Exp. With Flow Ind. Vib., Germany, Karlsruhe, University of Karlsruhe, 681-695.

Davenport, A.G. 1964. Note on the Distribution of the Largest Value of a Random Function with Application to Gust Loading, Proc. Inst. Civil Eng., 187-196.

Engineering Standard Data Unit (ESDU). 1984. ESDU 83045 – Strong Winds in the Atmospheric Boundary Layer: Part 2: Discrete Gust Speeds, ESDU International Inc.

FEMA. 2012. Seismic Performance Assessment of Buildings, FEMA P-58.

Fujino, Y., Wilde, K., Masukawa, J. and Bhartia, B. 1995. Rational Function Approximation of Aerodynamic Forces on Bridge Deck and Its Application to Active Control of Flutter. Proceedings of the 9th International Conference on Wind Engineering, New Delhi, India.

Griffis, L., Patel, V., Muthukumar, S. and Baldava, S. 2012. A Framework for Performance-Based Wind Engineering. Proceedings of the ATC-SEI Advances in Hurricane Engineering Conference, Miami, FL.

Gu, M. and Quan, Y. 2004. Across-wind Loads on Typical Tall Buildings. J. Wind Eng. and Ind. Aerodyn. 92: 1147-1165.

Holmes, J.D. 2001. Wind Loading of Structures, E & FN Spon, London.

Holmes, J.D. 1996. Along-wind Response of Lattice Towers –II: Aerodynamic Damping and Deflection. Eng. Struct., 18: 483-488.

International Standards Organization (ISO) 6897-1984: Guidelines for the Evaluation of the Response of Occupants of Fixed Structures, Especially Buildings and Off-shore Structures, to Low Frequency Horizontal Motion (0.063 to 1 Hertz).

Isyumov, N. 1995. Motion Perception, Tolerance and Mitigation. Proceedings of the 5th World Congress of the Council on Tall Buildings and Urban Habitat, Amsterdam, The Netherlands.

Isyumov, N. 1993. Criteria for Acceptable Wind-induced Motions of Tall Buildings. Proceedings of the International Conference on Tall Buildings, Council on Tall Buildings and Urban Habitat, Rio de Janerio, Brazil.

Jeong, U.Y. 2015. Advances in Tall Building Design under Strong Winds. Structures Congress 2015, ASCE/SEI.

Judd, J.P. and Charney, F.A. 2016. Wind Performance Assessment of Buildings. Geotechnical and Structural Engineering Congress 2016, ASCE, 1259-1268.

Judd, J.P. and Charney, F.A. 2015. Inelastic Building Behavior and Collapse Risk for Wind Loads. Proc., Structures Congress 2015, ASCE, Reston, Virginia.

Kareem, A. 1990. Reduction of Wind Induced Motion Utilizing a Tuned Sloshing Damper. J. of Wind Engineering and Industrial Aerodynamics, 36: 725-737.

Kareem, A. and Sun, W.J. 1987. Stochastic Response of Structures with Fluid-containing Appendages. J. of Sound and Vibration, 119(3).

Katagiri, J., Ohkuma, T., Marukawa, H. and Shimomura, S. 2000. Motion-induced Wind Forces Acting on Rectangular High-rise Buildings with Side Ratio of 2. J. Struct. Constr. Eng., AIJ 534: 25-32.

Larsen, R., Klemencic, R., Hooper, J. and Aswegan, K. 2016. Engineering Objectives for Performance-Based Wind Design. Geotechnical and Structural Engineering Congress 2016, ASCE, 1245-1258.

Nakai, M. Hirakawa, K., Yamanaka, M., Okuda, H., and Konishi, A. 2013. Performance-Based Wind-Resistant Design for High-rise Structures in Japan. International Journal of High-Rise Buildings, 2: 271-283.

NOAA, Climate Data Online, Retrieved from https://www.ncdc.noaa.gov/.

Pacific Earthquake Engineering Research Center (PEER). 2010. Guidelines for Performance-Based Seismic Design of Tall Buildings. PEER, College of Engineering, U.C. Berkeley.

Randall, R.B., 1987. Frequency Analysis, Brüel & Kjær.

Solari, G. 1993a. Gust Buffeting. I: Peak Wind Velocity and Equivalent Pressure. Journal of Structural Engineering, 119(2): 365-382.

Solari, G. 1993b. Gust Buffeting. II: Dynamic Alongwind Response. Journal of Structural Engineering, 119(2): 383-398.

Steckly, A. 1989. Ph.D. Thesis, University of Western Ontario.

Watanabe, Y., Isyumov, N. and Davenport, A.G. 1997. Empirical Aerodynamic Damping Function for Tall Buildings. J. of Wind Eng. and Ind. Aerodynamics, 72: 313-321.